At lower levels, when the percentage difference between the upward and downward flux becomes much larger, the net flux becomes easier to measure. Near the surface, the ratio between upward and downward flux approaches 6, and the net flux is essentially known to the accuracy of the downward flux alone. At present, we believe that the individual fluxes are known to an absolute accuracy of about 15 percent and that the upward and downward fluxes are each known relative to each other to about ±2 percent.

Together, the three sources of uncertainty in absolute response, relative response, and nonflat spectral response probably result in less than 20 percent uncertainty in the net flux near the surface and less than 40 percent uncertainty at high altitudes. The systematic uncertainties affect the net flux profile in predictable ways. Because the statistical noise in the data is small, the features in the curve are well established. As we continue to refine the calibration and particularly as the data at the highest altitudes become available and are tied to ground-based and orbiter data from outside the atmosphere, these uncertainties should be reduced.

Several interesting features are apparent in Fig. 2. At pressures greater than 1.3 atm, the variation of upward and downward flux with depth is very smooth and slow in contrast to the situation at lower pressures. Detailed inspection of the low-pressure region indicates excellent correlation of the rate of flux decrease with the measurement of cloud layers by the cloud particle size spectrometer (*3*) and the nephelometer experiments (*4*). In particular, three different rates of flux decrease are seen between 1.03 and 1.3 atm, 0.32 and 0.97 atm, and less than 0.32 atm. The clouds at pressures greater than 0.32 atm absorb remarkably little sunlight.

The flux profiles at pressures greater than 1.3 atm are consistent with that expected for a Rayleigh scattering atmosphere with a small amount of absorption. The upward and downward fluxes are very different at our lowest measurement levels, implying a ground albedo less than about 15 percent in the visible.

The solar constant at Venus of about 2600 W/m^2 implies a downward solar flux incident at the top of the atmosphere at the entry site (~67° solar zenith angle) of about 1000 W/m^2. Model calculations we have made that are consistent with the spherical albedo of Venus give a bolometric net solar flux at the top of the atmosphere of roughly 180 W/m^2 at this solar zenith angle. About half of this 180 W/m^2 is absorbed above the 185-mbar level. Fig. 2 gives the net flux profile below this level for the wavelength regions shown. About 15 W/m^2 in the 0.4- to 1.0-μm region are absorbed at the ground. We calculate that the planet-wide average flux profile is about 20 percent less than the flux profile measured at 67° solar zenith angle. Averaged over the entire planet, some 12W/m^2 are absorbed at the ground. The fraction of the incident solar energy that is absorbed at the ground is thus about $(4\pi R_v^2 \times 12$ W/m$^2)/(\pi R_v^2 \times 2600$ W/m$^2)$, or about 2 percent.

Accurate measurement of the solar energy deposition profile provides data essential for determining the effectiveness of the greenhouse mechanism. Although we have not yet completed detailed calculations based on these measurements, some evidence already exists that the greenhouse mechanism will support a high surface temperature. Calculations by Pollack and Young (*5*) based on Venera data in which some 1 percent of the incident sunlight reached the ground have been able to give high surface temperatures for some assumption of thermal opacity. These measurements should allow the greenhouse to work even with slightly lower thermal opacity.

In addition to further work to refine our instrumental calibration, we plan theoretical studies in three areas. First, we intend to model the angular distribution of the measured intensities for a wide range of optical properties in the clouds. We hope to derive not only the optical depths of the cloud layers but also the single scattering albedos and phase functions of the cloud particles. Second, we plan to continue our model calculations of solar deposition at a variety of solar zenith angles to refine the factors used to scale our measurements to planet-wide averages. Finally, we have begun a series of globally averaged greenhouse model calculations to investigate the temperature profiles that our net flux profiles imply for various sources of thermal opacity.

M. G. TOMASKO, L. R. DOOSE
J. PALMER, A. HOLMES
W. WOLFE, N. D. CASTILLO
P. H. SMITH
Lunar and Planetary Laboratory
and *Optical Science Center,*
University of Arizona, Tucson 85721

References and Notes

1. M. G. Tomasko *et al. Space Sci. Rev.* **20,** 389 (1977).
2. L. Colin and D. M. Hunten, *ibid.*, p. 468.
3. R. G. Knollenberg and D. M. Hunten, *Science*, **203,** 792 (1979).
4. B. Ragent and J. Blamont, *ibid.*, p. 790.
5. J. B. Pollack and R. Young, *J. Atmos. Sci.* **32,** 1025 (1975).
6. A. Seiff (1978), personal communication.
7. We are especially indebted to several individuals for the success of this experiment, including the late Dr. A. E. Clements for his many contributions to the original design of the experiment; L. Thane and K. Schlichtemeyer of the Martin Marietta Corporation for the outstanding performance of the LSFR electronics; and J. Ferandin and his colleagues at NASA-Ames Research Center for delivering a data tape so rapidly after Venus entry.

16 January 1979

First Results from the Large Probe Infrared Radiometer Experiment

Abstract. *During the descent to the surface of Venus, the large probe infrared radiometer measured the net thermal radiative flux in several spectral bandpasses. Preliminary analysis has permitted us to estimate (i) the infrared extinction coefficient profile attributable to aerosols, with respect to their visible profile, in the upper atmosphere of Venus and (ii) the water vapor mixing ratio below the clouds. An indication of the composition of a multicomponent cloud is seen in the data from the spectral bandpass from 6 to 7 micrometers.*

The objectives of the large probe infrared radiometer (LIR) experiment were to measure the net thermal flux and its divergence, to detect clouds and determine their infrared opacity, and to detect the presence of water vapor (and obtain an estimate of its abundance) during descent through the atmosphere of Venus. The instrument is a multichannel infrared radiometer that alternately measures the upward and downward radiation. The difference between these measurements, the net flux, constitutes the data that were transmitted to Earth. Descriptions of the hardware have been published elsewhere (*1, 2*). The nominal spectral bandpasses used were (i) for the net thermal flux, 3 to 150 μm, (ii) for cloud detection, 8 to 9 μm (a CO_2 "window"), and (iii) for water vapor, 6 to 7 and 7 to 8 μm.

At the present state of data reduction all indications are that the instrument itself functioned correctly throughout the mission. Tests covering the periods before the launch, during the cruise, and

0036-8075/79/0223-0797$00.50/0

before entry yielded noise and housekeeping data (temperatures and voltages) identical to those measured in earlier laboratory and calibration tests. During descent through Venus's atmosphere, all instrument voltages were stable and the measured temperature increases of the instrument were essentially those which had been predicted. (An early indication that the front of the instrument became extremely hot was subsequently shown to be incorrect.) The signals from the onboard calibration system (*1*) during the descent phase were also within nominal values.

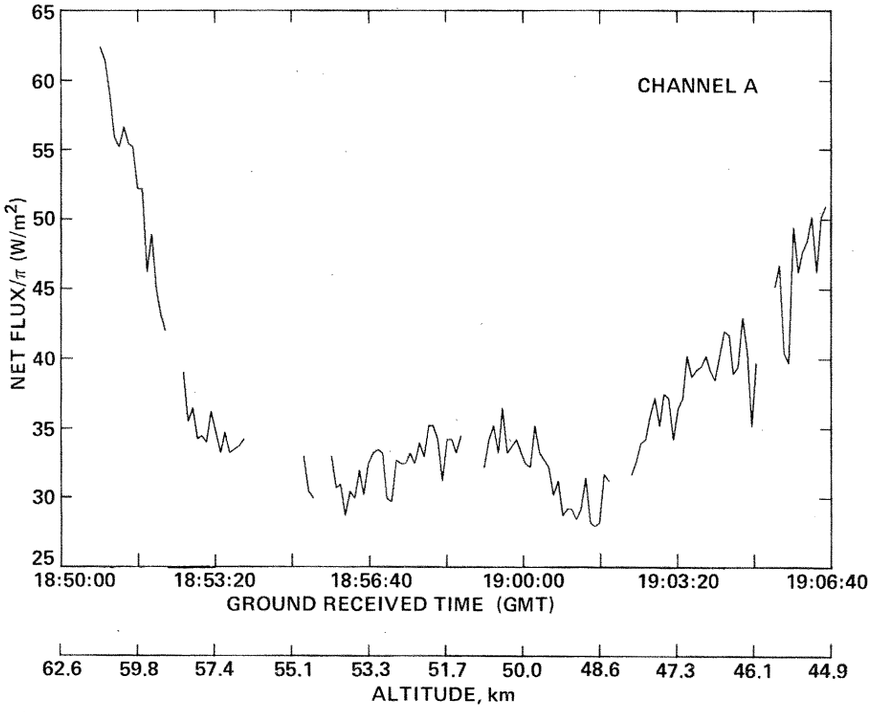

Fig 1. The observed net flux from the broad-band thermal channel from about 61 to 45 km. The short breaks in the curve are times when the instrument was in the calibrate mode. The longer gap, starting at about 57 km, represents a period for which data have not yet been received.

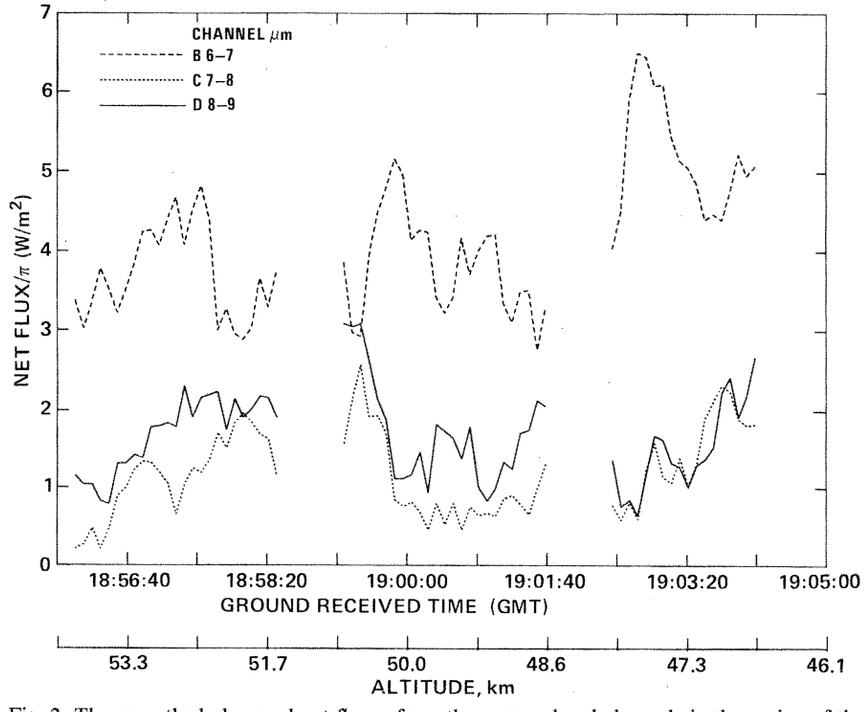

Fig. 2. The smoothed observed net fluxes from the narrow-band channels in the region of the bottom cloud.

The first data available for analysis were received at 1850:51 (ground receipt time, GMT); from preliminary data (*3*) this corresponds to an altitude of about 61 km (*4*). The net flux values appear reasonable until about 1906:20 (~ 45 km), at which time (which corresponds closely to that of parachute release), all data channels became noisy. Subsequently, until the impact on the surface, all channels produced signals that increased unreasonably. Expectations were that the net flux would steadily decrease to a low value. The cause of this anomaly has not yet been definitively identified. The data below 45 km appear to be recoverable, and first results of this effort are very promising. Since this process is not complete, however, we will address only the data from the upper atmosphere at this time.

In Fig. 1 we have displayed the net flux (upward flux minus downward flux) from the broad-band thermal channel. The net flux decreases rapidly at the earliest times, is relatively constant over a large altitude range, decreases slightly in about the altitude range of 50 to 47 km, and increases from about 47 to 45 km. The first decrease in the net flux is approximately a factor of 2 over a fraction of a scale height (~ 3 km). This indicates the presence of an additional source of thermal opacity besides CO_2, most probably extinction by particulates or droplets. In the second region, from about 57 to 50 km, the infrared absorption coefficient per unit length is approximately constant with altitude. The third region, which corresponds well to the "bottom cloud" reported by Knollenberg and Hunten (*5*), indicates enhanced thermal opacity for this broad wavelength channel; the net flux decreases by 15 to 20 percent. The increase in the net flux in the fourth region corresponds to that which would be expected if a "cool," relatively opaque source above the instrument (the cloud bottom) were subtracted from upward radiation, which increases with atmospheric temperature as the probe descends.

In Fig. 2 we present the net flux for the bottom cloud region as obtained from the three narrow-band channels, which have 1-μm bandwidths. These data have been smoothed with an unweighted, five-point moving average. This process causes a loss of 12 seconds of data at each end of a data cycle. At about 50.5 km, both channel D (the cloud detection channel) and channel C suddenly exhibit a de-

crease in the net flux and then recover slowly to their former levels. The sudden change corresponds nicely to the top of the bottom cloud. In both bandpasses, the change in the net flux is about a factor of 3, which implies a comparable increase in the extinction coefficient in these spectral regions. Because the spectral region at 7 to 9 μm corresponds to a CO_2 "window," the bottom cloud must be considered when investigating radiation leaks from Venus's atmosphere.

Channel B, the water vapor channel, exhibits flux changes different from those seen in the other narrow bandpass channels. The net flux decreases about 30 percent at about 52.25 km, before the bottom cloud is reached. In this wavelength interval, the net flux at the top of the bottom cloud suddenly increases and subsequently decreases about 50 percent within the cloud. A sharp increase, beginning about 48 km, occurs before the "normal" cloud bottom is reached. An explanation of this behavior is not available, but the data indicate the presence of two or more sources of opacity in this general altitude region.

We have started to interpret the results of this experiment by carrying out a number of theoretical simulations. We subdivided the infrared spectral region into 46 intervals and used the transmission average formalism of Pollack (*6*) to determine both the net flux (F) for the view angle of the LIR (F_{LIR}), and the angularly integrated value of the net flux (F_A), as a function of altitude in the Venus atmosphere. The net flux values so determined for each wavelength interval were subsequently weighted by the spectral response characteristics of each radiometer channel to obtain predicted net flux values. Allowance was made for the gaseous opacity of water vapor and carbon dioxide by using band model parameters (*7*), and for aerosol opacity, which, for these calculations, was assumed to be independent of wavelength and due only to absorption.

A number of quantities need to be specified in order to carry out a given simulation. The temperature-pressure-altitude profiles obtained by the atmospheric structure experiment on the large probe was used for altitudes below 60 km (*4*), whereas at higher altitudes, a synthesized model based on prior spacecraft results was used (*8*). The two profiles are in approximate accord near 60 km. A profile of the visible extinction coefficient was obtained from a combination of the results of the cloud particle size spectrometer on the large probe for altitudes below 60 km (*5*) and a synthesized model for higher altitudes (*9*). Values for the infrared extinction coefficients were found by scaling these visible values. As additional probe data are reduced, it will be possible to define the model parameters at higher altitudes directly rather than relying on other data. Finally, CO_2 was assumed to constitute virtually 100 percent of the atmosphere, whereas water vapor was assumed to have a mixing ratio of 10^{-6} above the main clouds (*10*), a constant mixing ratio, α_{H_2O}, below the main clouds, and a smoothly varying mixing ratio within the clouds. As a nominal value for α_{H_2O} we used 10^{-3} (*11*).

The view angle of the LIR was chosen so that the ratio, r, of F_A to F_{LIR}, had an almost constant value with altitude. Our

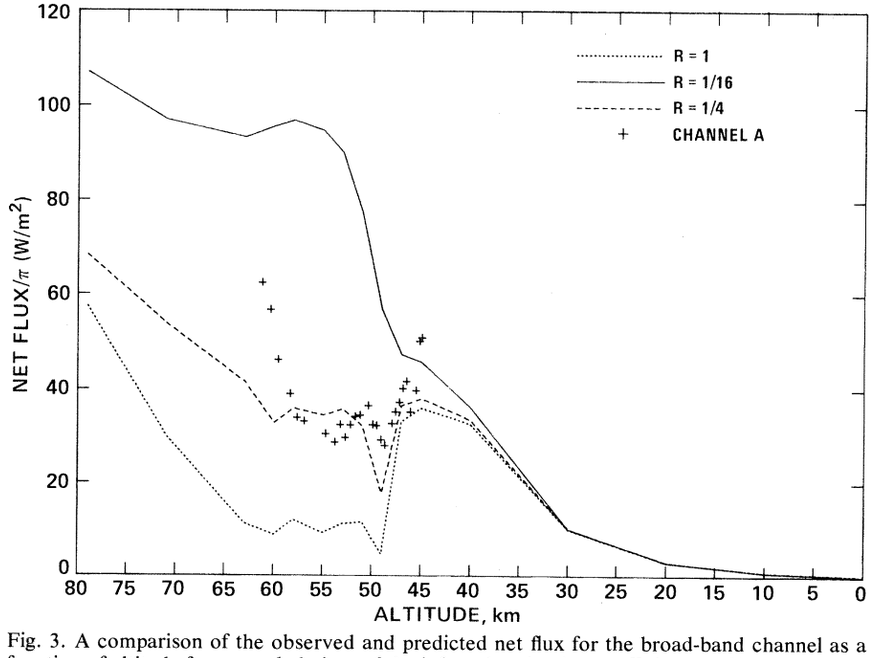

Fig. 3. A comparison of the observed and predicted net flux for the broad-band channel as a function of altitude for several choices of the infrared extinction coefficient profile, σ_{ir}, in relation to the visible extinction coefficient profile, σ_{vis}. $R = \sigma_{ir}/\sigma_{vis}$.

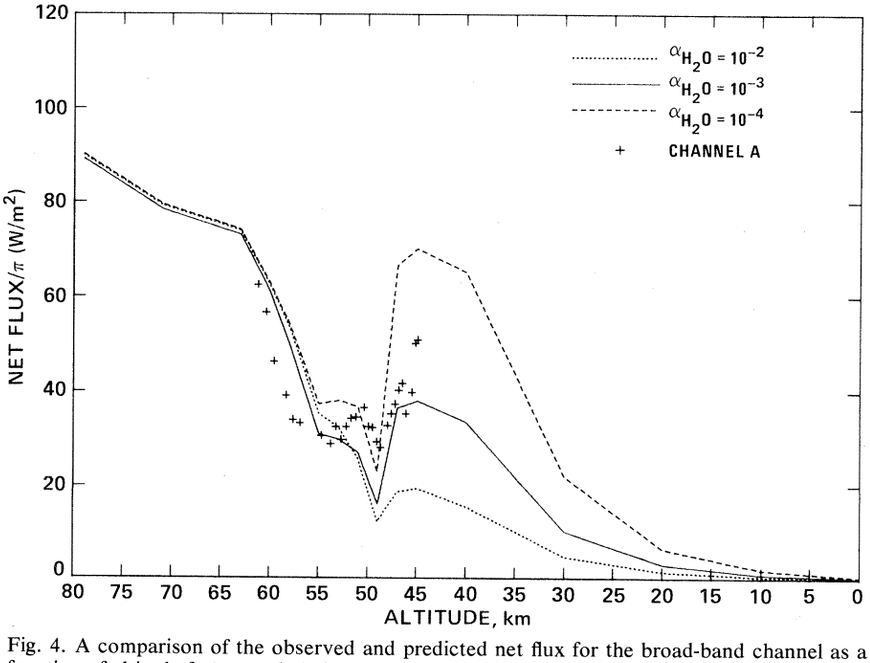

Fig. 4. A comparison of the observed and predicted net flux for the broad-band channel as a function of altitude for several choices of the water vapor mixing ratio below the main clouds, α_{H_2O}. For $\alpha_{H_2O} = 10^{-3}$ a somewhat different profile of the water vapor mixing ratio through the clouds was used than for the other runs. In all cases, $R = 1/16$ in the topmost cloud layer (above ~ 57 km) and $R = 1/4$ in the middle and bottom cloud layers.

best current atmospheric models indicate that r has a value of about 0.95 with a dispersion of about $\pm$ 0.03 and that r is almost independent of the model.

We have compared the theoretical calculations and the observations to obtain first-order estimates of the infrared opacity of the cloud particles and the water vapor mixing ratio beneath the clouds, α_{H_2O}. Figure 3 shows synthetic net flux profiles for the broad-band channel for three values of the infrared cloud opacity. The lower curve was computed for an infrared extinction coefficient profile, σ_{ir}, equal to the visible profile, σ_{vis}, whereas for the middle and upper curves $R = \sigma_{ir}/\sigma_{vis}$ equaled 1/4 and 1/16, respectively. Comparing these predictions with the observed values in the altitude range approximately 57 to 50 km, the location of the "middle cloud layer" (*5*), we conclude that in this cloud the observed $R \simeq 1/4$. This result seems reasonable since, in the longer wavelength region of the thermal infrared, the particle size (*5*) became small compared with the wavelength and thus we expect R to be less than 1.

For all the theoretical curves of Fig. 3, the net flux rises more slowly above 57 km, that is, in the region of the "upper cloud layer" (*5*), than does the observed profile. This difference indicates that R is significantly less than 1/4 in this cloud layer, a result consistent with the absence of large particles there. Also, the predicted decrease of the net flux within the bottom cloud layer, which spans the region from 50 to 47 km, is greater than is observed. Hence, while σ_{ir} increases from the middle to the bottom cloud layer, it does so by a smaller amount than at visible wavelengths. Analogous comparisons with the narrow-band results imply that σ_{ir} is somewhat larger in these channels than in the broad-band channel.

Figure 4 illustrates the sensitivity of the predictions to variations in the water vapor mixing ratio beneath the clouds, α_{H_2O}. Comparing these curves with the observed broad-band results below 47 km, the bottom of the main clouds, we see that a value of about 10^{-3} is required. This result is in approximate accord with other spacecraft data (*11*).

Finally, we consider the implications of the findings for the planetary heat balance. Averaged over the thermal infrared, the cloud system has an optical depth of about 7, which can be compared to a value of about 35 at visible wavelengths (*5, 9*). Thus, the clouds represent an important source of infrared opacity. We note that the amount of water vapor deduced to be present below the clouds is comparable to the amount needed to close the major CO_2 windows in the infrared and achieve the greenhouse effect (*7, 12*). Thus, the high surface temperature of Venus may be explained by the opacity of CO_2 and H_2O vapor, but with a significant assist from the cloud particles.

ROBERT W. BOESE
JAMES B. POLLACK
PETER M. SILVAGGIO
NASA Ames Research Center, Moffett Field, California 94305

References and Notes

1. L. Colin and D. Hunten, *Space Sci. Rev.* **20**, 471 (1977).
2. F. G. Brown, J. Gilland, R. Hassig, R. W. Boese, *SPIE J.* **126**, 95 (1977).
3. A. Seiff, personal communication.
4. ———, D. B. Kirk, S. Sommer, R. Young, R. Blanchard, D. Juergens, J. Lepetich, P. Intrieri, J. Findley, J. Derr, *Science* **203**, 787 (1979).
5. R. G. Knollenberg and D. M. Hunten, *ibid.*, p. 792.
6. J. B. Pollack, *Icarus* **10**, 301 (1969).
7. ——— and R. Young, *J. Atm. Sci.* **32**, 1025 (1975).
8. M. Ya Marov, *Icarus* **16**, 415 (1972).
9. A. Lacis, *J. Atm. Sci.* **32**, 1107 (1975).
10. E. S. Barker, *Icarus* **25**, 268 (1975).
11. V. I. Oyama, G. C. Carle, F. Woeller, J. B. Pollack, *Science* **203**, 802 (1979); V. I. Moroz, N. A. Parfent'ev, N. F. San'ko, V. S. Zhegulev, L. V. Zasova, E. A. Ustinov, *Cosmic Res.* **14**, 649 (1977).
12. J. B. Pollack, *Icarus* **10**, 314 (1969).
13. We thank C. Hall and his personnel in the Pioneer Project Office for all the assistance and attention given to this experiment. Special appreciation is expressed to R. Twarowski for the many hours he spent to help ensure this experiment's success. The LIR instrument was built at Ball Aerospace Systems Division, Boulder, Colo., under the direction of J. Gilland. The atmospheric modeling and programming work has benefited greatly by the efforts of A. Summers and B. Baldwin. The assistance of A. Aurelius, M. Liu, and J. Gibson in data processing is gratefully acknowledged.

16 January 1979

Venus Lower Atmospheric Composition: Preliminary Results from Pioneer Venus

Abstract. *Initial examination of data from the neutral mass spectrometer on the Pioneer Venus sounder probe indicates that the abundances of argon-36, argon-38, and neon-20 in the Venus atmosphere are much higher than those of the corresponding gases in Earth's atmosphere, although the abundance of radiogenic argon-40 is apparently similar for both planets. The lower atmosphere of Venus includes significant concentrations of various gaseous sulfur compounds. The inlet leak to the mass spectrometer was temporarily blocked by an apparently liquid component of the Venus clouds during passage through the dense cloud layer. Analysis of gases released during the evaporation of the droplets shows the presence of water vapor to some compound or compounds of sulfur.*

The sounder probe, or large probe, of the Pioneer Venus multiprobe spacecraft (*1*) entered the atmosphere of Venus on 9 December 1978. It carried seven instruments, including a neutral mass spectrometer, designed to measure the composition of the lower atmosphere of Venus.

The mass spectrometer, a single focusing magnetic sector device (*2*), was intended to measure atomic masses ranging from hydrogen to lead. Gases were admitted to the instrument through a set of two microleaks. The leaks were hermetically sealed prior to launch by means of a ceramic cap attached to a flange in the shell of the probe behind the heat shield. The cap was broken with a pyrotechnic device, exposing the leaks to the Venus atmosphere a few seconds after the parachute was deployed and the heat shield jettisoned. Gas molecules entering the leaks passed through an ion source where they could be ionized by electrons with an impact energy of 70 eV. The electron impact energy was reduced to 30 and 22 eV on successive mass scans on three occasions during descent, providing additional aids for the identification of parent molecules, whose cracking patterns change significantly as the ambient energy is reduced from 70 to 22 eV. Additional simplification of the spectrum occurs since the production of doubly charged ions is negligible at lower impact energies.

Ambient gases were removed from the ion source by a chemical getter. The pumping speed was controlled by a valve connecting the ion source and getter. The valve was allowed to open during descent in response to increasing atmospheric pressure, maintaining in this fashion a relatively constant pressure at the ion source (*3*). Preliminary flight data indicate that the pressure in the ion source responded as expected to changes in external pressure, increasing by less than a factor of 10 while the external pressure increased by a factor of 10^3. An anomaly occurred near 50 km in a region of the atmosphere where Knollenberg and Hunten (*4*) and Ragent and Blamont (*5*) detected the presence of sig-

0036-8075/79/0223-0800$00.50/0